

Recent demography drives changes in linked selection across the maize genome

Timothy M. Beissinger * † ‡, Li Wang § ¶, Kate Crosby *, Arun Durvasula *, Matthew B. Hufford §, and Jeffrey Ross-Ibarra * ||

*US Department of Agriculture, Agricultural Research Service, Columbia, MO, USA, †Division of Plant Sciences, University of Missouri, Columbia, MO, USA, ‡Dept. of Plant Sciences, University of California, Davis, CA, USA, §Department of Ecology, Evolution, and Organismal Biology, Iowa State University, Ames, IA, USA, ¶Genome Informatics Facility, Iowa State University, Ames, IA, USA, and ||Genome Center and Center for Population Biology, University of California, Davis, CA, USA

Submitted to Proceedings of the National Academy of Sciences of the United States of America

The genetic variability present in a population results from a constant interaction between drift and selection. To quantify the interplay between demography (which drives drift) and selection, we investigated genetic diversity in maize, one of the most important crops for food, feed, and fuel world-wide. Our sample included whole genome sequence data from 23 maize and 13 teosinte individuals. We obtained a complete estimate of the population size fluctuations and other demographic parameters experienced by maize as it was domesticated from teosinte. Here, we show that maize went through a domestication bottleneck with a population size of approximately 5% that of teosinte before it experienced rapid population size expansion post-domestication. We observe that hard sweeps on genic mutations are not the primary force driving maize evolution. We find that a reduced population size during domestication decreased the efficiency of purifying selection to purge deleterious alleles from maize. However, expansion after domestication has since increased the efficiency of purifying selection to levels exceeding those seen in teosinte. Our results demonstrate that demographic and selective history in the ancient and recent past both contribute to the levels of genetic variability that are present today. Our results also show that for bottlenecked species, rapid post-bottleneck expansion can have wide-ranging impacts on diversity that conflict with the expected loss of diversity that occurs during the bottleneck itself.

The genetic diversity of populations is determined by a constant interplay between genetic drift and selection. Drift is a consequence of a finite population size and the random sampling of gametes every generation [1]. In contrast to the stochastic effects of drift, selection systematically alters allele frequencies by favoring particular alleles at the expense of others as a result of their effects on fitness. Researchers often seek to study drift by excluding potentially selected sites [2–4], or to study selection by focusing on site-specific patterns under the assumption that genome-wide diversity reflects primarily the action of drift [5].

Drift and selection do not operate independently to determine genetic variability, however, in large part because linkage allows the effects of selection to be wide-ranging [6–8]. Linked selection can take the form of hitch-hiking, when the frequency of a neutral allele changes as a result of positive selection at a physically linked site [6], or background selection, where diversity is reduced at loci linked to a site undergoing selection against deleterious alleles [9]. Recent work in a *Drosophila*, for example, has shown that virtually the entire genome is impacted by the combined effects of these processes [10–12]. The impact of linked selection, in turn, is heavily influenced by the effective population size (N_e), as the efficiency of natural selection is proportional to the product $N_e s$, where s is the strength of selection on a variant [8, 13–15]. The effective size of a population is not static, and nearly all species, including flies [16], humans [17], domesticates [18, 19], and non-model species [20] have experienced recent or ancient changes in N_e . Although much is known about how the long-term average N_e affects linked selection, much less is understood about the im-

mediate effects and dynamics of changing in N_e on patterns of linked selection.

Because of its relatively simple demographic history and the abundant availability of genomic tools, maize (*Zea mays*) represents an excellent organism to study these effects. Maize is a species of tremendous importance worldwide as both a model species [21] and a staple crop [22]. Archaeological and genetic studies have established that maize domestication began in Central Mexico at least 9,000 years bp [23, 24], and involved a population bottleneck followed by recent expansion [25–27]. Because of this simple but dynamic demographic history, patterns of linked selection domesticated maize and its wild ancestor teosinte can be used to understand the effects of changing N_e on linked selection. Here, we leverage this system to study how recent demographic change impacts patterns of linked selection genome-wide. We begin by estimating the parameters of the maize domestication bottleneck using whole-genome resequencing data, then investigate the relative importance of different forms of linked selection on diversity in the recent and ancient past. We show that while patterns of overall nucleotide diversity reflect long-term differences in N_e ,

Significance

Both selection and demographic change play important roles in shaping diversity across the genome, but clear empirical examples of the interplay of these two forces are lacking. Here we document the combined effects of demography and linked selection on genome-wide diversity in domesticated maize and its wild ancestor teosinte. We estimate that maize underwent a bottleneck to $\approx 5\%$ of the size of the ancestral teosinte population, but that recent expansion has resulted in a maize population perhaps orders of magnitude larger than teosinte. We show that positive selection on new genic mutations has had relatively little effect on genetic diversity, but that selection against deleterious mutations has dramatically reduced diversity in and immediately around genes in both taxa. We find that the relative impact of selection depends on the age of the polymorphisms evaluated: while older polymorphisms in maize show more limited effects of linked selection, new mutations instead reflect its larger current size and more efficient selection. Our results demonstrate that a complete understanding of genome-wide patterns of diversity will require careful assessment of both demographic history and the effects of linked selection.

Reserved for Publication Footnotes

recent growth following domestication qualitatively changes these effects, illustrating the importance of understanding demographic history when considering the effects of selection on the genome.

Results

Patterns of diversity differ between genic and intergenic regions of the genome. To investigate how demography and linked selection have shaped patterns of diversity in maize and teosinte, we analyzed data from 23 maize and 13 teosinte genomes from the maize HapMap 2 and HapMap 3 projects [30,31]. As a preliminary step, we evaluated levels of diversity inside and outside of genes across the genome. We find broad differences in genic and intergenic diversity consistent with earlier results [32] (Figure 1). In maize, mean pairwise diversity (π) within genes was significantly lower than at sites at least 5

kb away from genes (0.00668 vs 0.00691 , $p < 2 \times 10^{-44}$). Diversity differences in teosinte are even more pronounced (0.0088 vs. 0.0115 , $p \approx 0$). Differences were also apparent in the site frequency spectrum, with mean Tajima's D positive in genic regions in both maize (0.4) and teosinte (0.013) but negative outside of genes (-0.087 in maize and -0.25 in teosinte, $p \approx 0$ for both comparisons). These observations suggest that diversity in genes is not evolving neutrally, but instead is reduced by the impacts of selection on linked sites.

Demography of maize domestication. After establishing that genic sites are not evolving neutrally, we used sites $> 5\text{kb}$ from genes to estimate the parameters of a simple domestication bottleneck model (Figure 2). The most likely model estimates an ancestral population mutation rate of $\theta = 0.0147$ per bp, which translates to an effective population size of $N_a \approx 123,000$ teosinte individuals. We estimate that maize split from teosinte $\approx 15,000$ generations in the past, with an initial size of only $\approx 5\%$ of the ancestral N_a . After its split from teosinte, our model posits exponential population growth in maize, estimating a final modern effective population size of $N_m \approx 370,000$. Maize and teosinte have continued to exchange migrants after the population split, with gene flow between the populations estimated at $M_{tm} = 1.1 \times 10^{-5} \times N_a$ migrants per generation from teosinte to maize and $M_{mt} = 1.4 \times 10^{-5} \times N_a$ migrants from maize to teosinte.

In addition to our simple bottleneck model, we investigated two alternative approaches for demographic inference. First, we utilized genotyping data from more than 4,000 maize landraces [28] to estimate the modern maize effective population size using low frequency variants informative of population expansion. This analysis yields a much higher estimate of the modern maize effective population size at $N_m \approx 993,000$. Finally, we applied a model-free coalescent approach [29] using a subset of our samples. Though this analysis suggests non-equilibrium dynamics for teosinte not included in our initial model, it is nonetheless broadly consistent, identifying a clear domestication bottleneck followed by rapid population expansion in maize to an extremely large extant size of $\approx 10^9$ (Figure S2).

Diversity is strongly influenced by purifying selection. In the case of purifying or background selection, diversity can be reduced in functional regions of the genome via removal of deleterious mutations [9]. We investigated purifying selection in

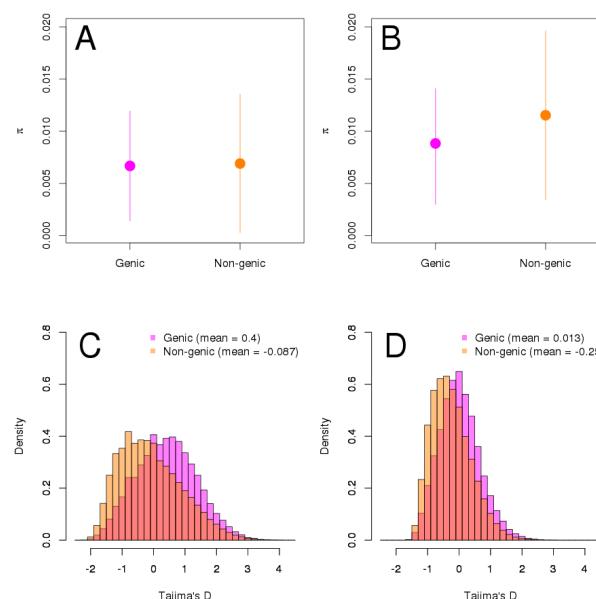


Fig. 1. Pairwise diversity π (A,B) and Tajima's D (C,D) in 1kb windows from genic and nongenic regions of maize (A,C) and teosinte (B,D). Shown in A and B are means and one standard deviation.

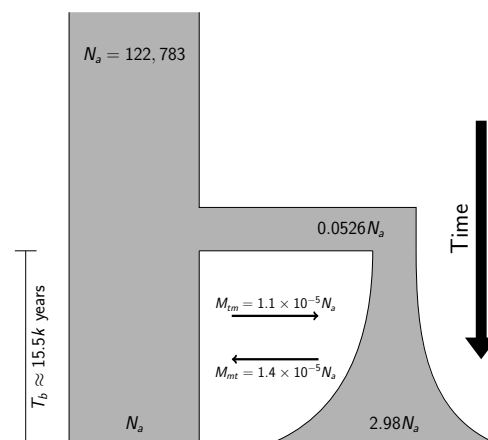


Fig. 2. Parameter estimates for a basic bottleneck model of maize domestication. See methods for details.

maize and teosinte by evaluating the reduction of diversity around genes. Pairwise diversity is strongly reduced within genes for both maize and teosinte (Figure 3A) but recovers quickly at sites outside of genes, consistent with the low levels of linkage disequilibrium generally observed in these subspecies [30, 33]. The reduction in relative diversity is more pronounced in teosinte, reaching lower levels in genes and occurring over a wider region.

Our comparison of synonymous and missense substitutions has low power to detect the effects of selection acting on multiple mutations or standing genetic variation, because in such cases diversity is not necessarily reduced [34, 35]. Such "soft

sweeps" are still expected to occur more frequently in functional regions of the genome and could provide an alternative explanation for the observed reduction of diversity in genes. To test this possibility, we performed a genome-wide scan for selection using the H12 statistic, a method expected to be sensitive to both hard and soft sweeps [36]. Qualitative differences between maize and teosinte remained unchanged even after removing genes in the top 20% of H12 (Figure S6A). We interpret these combined results as suggesting that purifying selection has left a more pronounced signature in the teosinte genome due to the increased efficacy of selection resulting from differences in effective population size.

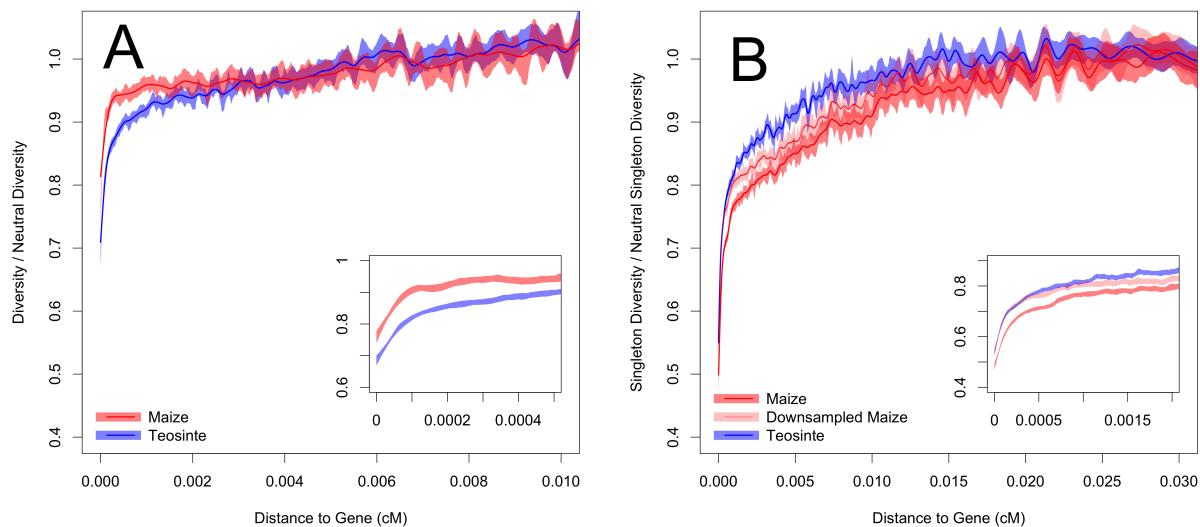


Fig. 3. Relative diversity versus distance to nearest gene in maize and teosinte. Shown are **A** pairwise nucleotide diversity and **B** singleton diversity. Relative diversity is calculated compared to the mean diversity in windows $\geq 0.01\text{cM}$ or $\geq 0.02\text{cM}$ from the nearest gene for pairwise diversity and singletons, respectively. Lines depict cubic smoothing splines with smoothing parameters chosen via generalized cross validation and shading depicts bootstrap-based 95% confidence intervals. Inset plots depict a smaller range on the x-axis.

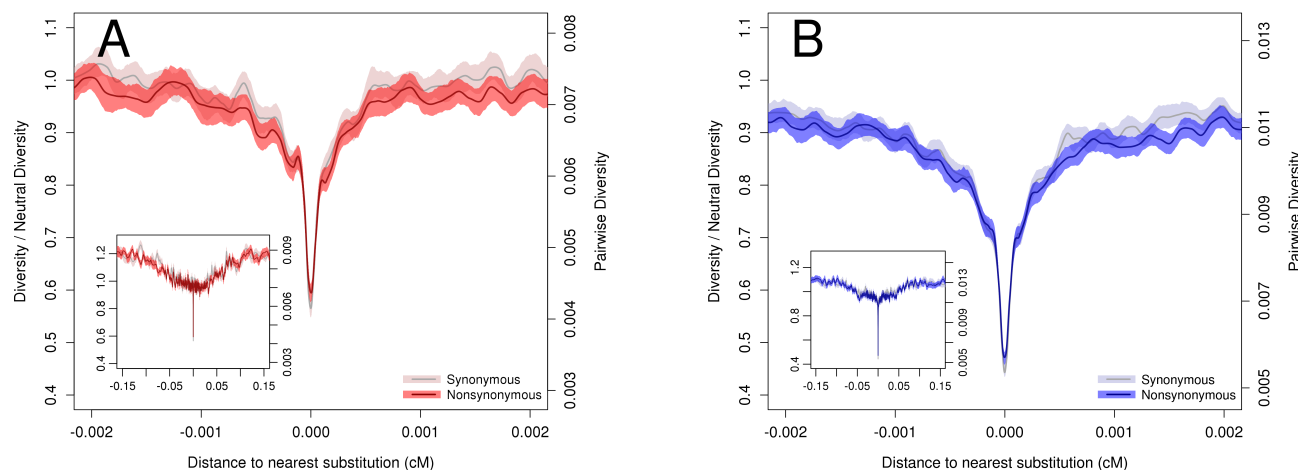


Fig. 4. Pairwise diversity surrounding synonymous and missense substitutions in **A** maize and **B** teosinte. Axes show absolute diversity values (right) and values relative to mean nucleotide diversity in windows $\geq 0.01\text{cM}$ from a substitution (left). Lines depict a loess curve (span of 0.01) and shading represents bootstrap-based 95% confidence intervals. Inset plots depict a larger range on the x-axis.

Population expansion leads to stronger purifying selection in modern maize. Motivated by the rapid post-domestication expansion of maize evident in our demographic analysis, we reasoned that low-frequency — and thus younger — polymorphisms might show patterns distinct from pairwise diversity. Singleton diversity around missense and synonymous substitutions (Figure S4) appears nearly identical to results from pairwise diversity (Figure 4), providing little support for a substantial increase in the number or strength of hard sweeps occurring in maize. In contrast, we observe a significant shift in the effects of purifying selection: singleton polymorphisms are more strongly reduced in and near genes in maize than in teosinte (Figure 3B), even after downsampling our maize data to account for differences in sample size. This result is the opposite of the pattern observed for π , where teosinte demonstrated a stronger reduction of diversity in and around genes than did maize. As was the case when we analyzed π , this relationship remained after we removed the 20% of genes with the highest H12 values (Figure S6). Finally, while direct comparison of pairwise and singleton diversity within taxa are consistent with at least some non-equilibrium dynamics in teosinte, as indicated by our coalescent-based demographic analysis, these too reveal much stronger differences in maize (Figure S5).

Hard sweeps do not explain diversity differences. When selection increases the frequency of a new beneficial mutation, a signature of reduced diversity is left at surrounding linked sites [6]. To evaluate whether patterns of such “hard sweeps” could explain observed differences in diversity between genic and intergenic regions of the genome, we compared diversity around missense and synonymous substitutions between *Trip-sacum* and either maize or teosinte. If a proportion of missense mutations have been fixed due to hard sweeps, diversity around these substitutions should be lower than around synonymous substitutions. We observe this pattern around the causative amino acid substitution in the maize domestication locus *tga1* (Figure S1), likely the result of a hard sweep during domestication [37,38]. Genome-wide, however, we observe no differences in diversity between synonymous and missense substitutions in either maize or teosinte (Figure 4).

Previous analyses have suggested that this approach may have limited power because a relatively high proportion of missense substitutions will be found in genes that are under weak purifying selection and thus have higher genetic diversity [39]. To address this concern, we took advantage of genome-wide estimates of evolutionary constraint [40], calculated using genomic evolutionary rate profile (GERP) scores [41]. We then evaluated substitutions only in subsets of genes in the highest and lowest 10% quantile of mean GERP score, putatively representing genes under the strongest and weakest purifying selection. As expected, we see higher diversity around substitutions in genes under weak purifying selection, but we still find no difference between synonymous and missense substitutions in either subset of the data (Figure S3). Taken together, these data suggest hard sweeps do not play a major role in patterning genic diversity in either maize or teosinte.

Discussion

Hard sweeps do not shape genome-wide diversity in maize. Our findings demonstrate that classic hard selective sweeps have not contributed substantially to genome-wide patterns of diversity in maize, a result we show is robust to concerns about power due to the effects of background selection [39]. Although our approach ignores the potential for hard sweeps in

noncoding regions of the genome, a growing body of evidence argues against hard sweeps as the prevalent mode of selection shaping maize variability. Among well-characterized domestication loci, only the gene *tga1* shows evidence of a hard sweep on a missense mutation [38], while several loci are consistent with “soft sweeps” from standing variation [42,43] or multiple mutations [44]. Moreover, genome-wide studies of domestication [32], local adaptation [45] and modern breeding [46] all support the importance of standing variation and/or non-coding variants as primary sources of adaptive variation. Soft sweeps are expected to be common when $2N_e\mu_b \geq 1$, where μ_b is the mutation rate of beneficial alleles with selection coefficient s_b [35]. Assuming a mutation rate of 3×10^{-8} [47] and that on the order of $\approx 1 - 5\%$ of mutations are beneficial [48], this implies that soft sweeps should be common in both maize and teosinte for mutational targets $>> 10kb$ — a plausible size for quantitative traits or for regulatory evolution targeting genes with large up- or down-stream control regions [42, e.g.]. Indeed, many adaptive traits in both maize [49] and teosinte [50] are highly quantitative, and adaptation in both maize [32] and teosinte [51] has involved selection on regulatory variation.

The absence of evidence for a genome-wide impact of hard sweeps differs markedly from observations in *Drosophila* [52] and *Capsella* [53], but is consistent with data from humans [54, 55]. [14] recently showed that selection tends to have an elevated impact reducing diversity in species with large population size compared to small, which may explain why maize and humans, both bottlenecked species, show similar patterns while *drosophila* and *capsella* behave differently.

Demography of domestication. Although a number of authors have investigated the demography of maize domestication [25–27], these efforts relied on data only from genic regions of the genome and made a number of limiting assumptions about the demographic model. We show that diversity within genes has been strongly reduced by the effects of linked selection, such that even synonymous polymorphisms in genes are not representative of diversity at unconstrained sites. This implies that genic polymorphism data are unable to tell the complete or accurate demographic history of maize, but the rapid recovery of diversity outside of genes demonstrates that sites far from genes can be reasonably used for demographic inference. Furthermore, by utilizing the full joint SFS, we are able to estimate population growth, gene flow, and the strength of the domestication bottleneck without requiring assumptions about its duration.

One surprising result from our model is the estimated timing of domestication at $\approx 15,000$ years before present. While this appears to conflict with archaeological estimates [56], we emphasize that this estimate reflects the fact that the genetic split between populations likely preceded anatomical changes that can be identified in the archaeological record. We also note that our result may also be inflated due to population structure, as our geographically diverse sample of teosinte may include populations diverged from those that gave rise to maize.

The estimated bottleneck of $\approx 5\%$ of the ancestral teosinte population seems low given that maize landraces exhibit $\approx 80\%$ of the diversity of teosinte [32], but our model suggests that the effects of the bottleneck on diversity are likely ameliorated by both gene flow and rapid population growth (Figure 2). Although we estimate that the modern effective size of maize is larger than teosinte, the small size of our sample reduces our power to identify the low frequency alleles most sensitive to rapid population growth [57], and our model is unable to incorporate growth faster than exponential. Both alternative approaches we employ estimate a much larger mod-

ern effective size of maize in the range of $\approx 10^6 - 10^9$, an order of magnitude or more than the current size of teosinte. Census data suggest these estimates are plausible: there are 47.9 million ha of open-pollinated maize in production [58], likely planted at a density of $\approx 25,000$ individuals per hectare [59]. Assuming the effective size is only $\approx 0.4\%$ of the census size (i.e. 1 ear for every 1000 male plants), this still implies a modern effective population size of more than four billion. While these genetic and census estimates are likely inaccurate, all of the evidence points to the fact that the effective size of modern maize is extremely large.

Demography influences the efficiency of purifying selection.

One of our more striking findings is that the impact of purifying selection on maize and teosinte variability has varied through time. Although we observe a more pronounced decrease in π around genes in teosinte than maize (Figure 3A), we see a greater decrease in singleton diversity in maize than teosinte (Figure 3B). Purifying selection is more efficient in larger populations [60], and our observations using π are thus consistent with our demographic model and previous work [25–27, 61] which shows a smaller long-term effective population size in maize. Similarly, our observations based on singleton diversity, which thereby reflect more recent patterns of selection, again are in agreement with maize and teosinte demography; from the viewpoint of a recent mutation, the rapid expansion of maize post-domestication means that today maize has a vastly larger effective population size than does teosinte.

A consequence of the previously-inefficient purifying selection in maize is that it likely harbors more weakly deleterious alleles segregating at intermediate frequency than does teosinte. Therefore, high genetic load could be a part of the explanation of why maize inbreds have continued to improve over the past several decades [62]. Our results also demonstrate that recent purifying selection in maize has become much more effective, potentially explaining the ongoing improvement of these inbreds as maize lines are continuously selected. Additionally, the large N_e of modern maize compared to modern teosinte implies that for new mutations, selection will operate much more efficiently in maize. This observation is not restricted to maize. Bottlenecks have been documented or predicted across most domesticated plant and animal species [18, 19, 63–65], but rapid expansion post-bottleneck, which we demonstrate generates ubiquitous consequences relating to genetic diversity, is not well studied. In human, model, and other species, these results demonstrate that observed patterns of selection depend heavily on recent and/or ancient patterns of demography.

Materials and Methods

BASH, R, and Python scripts. All scripts used for analysis are available in an online repository at [REPO ADDRESS HERE](#).

Plant materials. We made use of published sequences from inbred accessions of teosinte (*Z. mays* ssp. *parviglumis*) and maize landraces from the Maize HapMap3 panel as part of the Panzea project [30, 31, 66]. From these data, we removed 4 teosinte individuals that were not ssp. *parviglumis* or appeared as outliers in an initial principal component analysis conducted with the package adegenet [67] (Figure S7), leaving 13 teosinte and 23 maize that were used for all subsequent analyses (Table S8). We also utilized a single individual of (*Tripsacum dactyloides*) as an outgroup. All bam files are available at [/plant/home/shared/panzea/hapmap3/bam_internal/v3.bams.bwamem](#).

Physical and genetic maps. Sequences were mapped to the maize B73 version 3 reference genome [68] (ftp://ftp.ensemblgenomes.org/pub/plants/release-22/fasta/zea_mays/dna/) as described by [31]. All analyses made use of uniquely mapping reads with mapping quality score ≥ 30 and bases with base quality score ≥ 20 ; quality scores around indels were adjusted following Li *et al.* [69]. We converted physical coordinates to genetic coordinates via linear interpolation of the previously published 1cM resolution NAM genetic map [70].

Estimating the site frequency spectrum. We estimated both the genome-wide site frequency spectrum (SFS) as well as a separate SFS for genic (within annotated transcript) and intergenic ($\geq 5kb$ from a transcript) regions. We used the biomaRt package [71, 72] of R [73] to parse annotations from genebuild version 5b of AGPv3. We estimated single population and joint SFS with the software ANGSD [74], including all positions with at least one aligned read in $\geq 80\%$ of samples in one or both populations. We assumed individuals were fully inbred and treated each line as a single haplotype. Because ANGSD cannot calculate a folded joint SFS, we first polarized SNPs using the maize reference genome and then folded spectra using $\delta\alpha\delta i$ [4].

Demographic inference. We used the software $\delta\alpha\delta i$ [4] to estimate parameters of a domestication bottleneck from the joint maize-teosinte SFS, using only sites $> 5kb$ from a gene to ameliorate the effects of linked selection. We modeled a teosinte population of constant effective size N_a , that at time T_b generations in the past gave rise to a maize population of size N_b which grew exponentially to size N_m in the present (Figure 2). The model includes migration of M_{mt} individuals each generation from maize to teosinte and M_{tm} individuals from teosinte to maize. We estimated N_a using $\delta\alpha\delta i$'s estimation of $\theta = 4N_a\mu$ from the data and a mutation rate of $\mu = 3 \times 10^{-8}$ [47]. We estimated all other parameters using 1,000 $\delta\alpha\delta i$ optimizations and allowing initial values between runs to be randomly perturbed by a factor of 2. Optimized parameters along with their initial values and upper and lower bounds can be found in table S9. We report parameter estimates from the optimization run with the highest log-likelihood.

We further made use of a large genotyping data set of more than 4,000 maize landraces [28] to estimate the modern maize N_e from singleton counts. We filtered these data to include only SNPs with data in $\geq 1,500$ individuals, and then projected the SFS down to a sample of 500 individuals by sampling each marker without replacement 1,000 times according to the observed allele frequencies. We then estimated N_e from the data assuming $\mu = 3 \times 10^{-8}$ [47] and the relation $4N_e\mu = \frac{S}{L}$ [75], where where S is the total number of singleton SNPs and L is the total number of SNPs in the dataset.

As a final estimate of demography, we employed MSMC [29] to complement our model-based demographic inference. We used six each of maize and teosinte (BKN022, BKN025, BKN029, BKN030, BKN031, BKN033, TIL01, TIL03, TIL09, TIL10, TIL11 and TIL14), treating each inbred genome as a single haplotype. We called SNPs in ANGSD [74] using a SNP p-value of $1e-6$ against a reference genome masked using SNPable(). We then removed heterozygous genotypes and filtered sites with a mapping quality < 30 , a base quality < 20 , or a $|\log_2(depth)| < 1$. We ran MSMC with pattern parameters $20 \times 2 + 20 \times 4 + 10 \times 2$.

Diversity. We made use of the software ANGSD [74] for diversity calculations and genotype calling. We calculated diversity statistics in maize and teosinte in 1 kb non-overlapping windows using filters as described above for the SFS. We used allele counts to estimate the number of singleton polymorphisms in each window, and used binomial sampling to create a second maize data set down-sampled to have the same number of samples as teosinte. We called genotypes in maize, teosinte, and *Tripsacum* at sites with a SNP p-value $< 10^{-6}$ and when the genotype posterior probability > 0.95 . We identified substitutions in maize and teosinte as all sites with a fixed difference with *Tripsacum* and $\leq 20\%$ missing data. Substitutions were classified as synonymous, missense, or noncoding using the ensemble variant effects predictor [76]. For each window with $\geq 100bp$ of data we computed the genetic distance between the window center and the nearest synonymous and missense substitution as well as the genetic distance to the center of the nearest gene transcript.

Selection scan. We scanned the genome to identify sites that have experienced recent positive selection using the H12 statistic [36] in sliding windows of 200 SNPs with a step of 25 SNPs.

ACKNOWLEDGMENTS. We are indebted to Graham Coop and Simon Aeshbacher for their constructive input during this study. We thank Robert Bukowski and Qi Sun for providing early-access data from maize HapMap3. Funding was provided by NSF Plant Genome Research Project 1238014.

1. Dobzhansky, T & Pavlovsky, O. (1957) *Evolution* pp. 311–319.
2. Voight, B. F., Adams, A. M., Frisse, L. A., Qian, Y., Hudson, R. R., & Di Rienzo, A. (2005) *Proceedings of the National Academy of Sciences of the United States of America* 102, 18508–18513.
3. Luikart, G., England, P. R., Tallmon, D., Jordan, S., & Taberlet, P. (2003) *Nature Reviews Genetics* 4, 981–994.
4. Gutenkunst, R. N., Hernandez, R. D., Williamson, S. H., & Bustamante, C. D. (2009) *PLoS genetics* 5, e1000695.
5. Akey, J. M. (2009) *Genome research* 19, 711–722.
6. Smith, J. M. & Haigh, J. (1974) *Genetical research* 23, 23–35.
7. Li, J., Li, H., Jakobsson, M., Li, S., Sjödin, P., & Lascoux, M. (2012) *Molecular Ecology* 21, 28–44.
8. Slotte, T. (2014) *Briefings in functional genomics* 13, 268–275.
9. Charlesworth, B., Morgan, M., & Charlesworth, D. (1993) *Genetics* 134, 1289–1303.
10. Sella, G., Petrov, D. A., Przeworski, M., & Andolfatto, P. (2009) *PLoS genetics* 5, e1000495.
11. Elyashiv, E., Sattath, S., Hu, T. T., Strutovsky, A., McVicker, G., Andolfatto, P., Coop, G., & Sella, G. (2014) arXiv preprint arXiv:1408.5461.
12. Andolfatto, P. (2005) *Nature* 437, 1149–1152.
13. Cutter, A. D. & Payseur, B. A. (2013) *Nature Reviews Genetics* 14, 262–274.
14. Corbett-Detig, R. B., Hartl, D. L., & Sackton, T. B. (2015) *PLoS Biol* 13, e1002112.
15. Leffler, E. M., Bullaughey, K., Matute, D. R., Meyer, W. K., Segurel, L., Venkat, A., Andolfatto, P., & Przeworski, M. (2012) *PLoS Biol* 10, e1001388.
16. Duchen, P., Živković, D., Hutter, S., Stephan, W., & Laurent, S. (2013) *Genetics* 193, 291–301.
17. Reich, D. E. & Goldstein, D. B. (1998) *Proceedings of the National Academy of Sciences* 95, 8119–8123.
18. Hyten, D. L., Song, Q., Zhu, Y., Choi, I.-Y., Nelson, R. L., Costa, J. M., Specht, J. E., Shoemaker, R. C., & Cregan, P. B. (2006) *Proceedings of the National Academy of Sciences* 103, 16666–16671.
19. Consortium, B. H. et al. (2009) *Science* 324, 528–532.
20. Ellegren, H. (2014) *Trends in ecology & evolution* 29, 51–63.
21. Strable, J. & Scanlon, M. J. (2009) *Cold Spring Harbor Protocols* 2009, pdb-emo132.
22. Shifraw, B., Prasanna, B. M., Hellin, J., & Bänziger, M. (2011) *Food Security* 3, 307–327.
23. Smith, B. D. (1995) *The emergence of agriculture*. (Scientific American Library New York).
24. Matsuo, Y., Vigouroux, Y., Goodman, M. M., Sanchez, J., Buckler, E., & Doebley, J. (2002) *Proceedings of the National Academy of Sciences* 99, 6080–6084.
25. Wright, S. I., Bi, I. V., Schroeder, S. G., Yamasaki, M., Doebley, J. F., McMullen, M. D., & Gaut, B. S. (2005) *Science* 308, 1310–1314.
26. Eyre-Walker, A., Gaut, R. L., Hilton, H., Feldman, D. L., & Gaut, B. S. (1998) *Proceedings of the National Academy of Sciences* 95, 4441–4446.
27. Tenaillon, M. I., U'Ren, J., Tenaillon, O., & Gaut, B. S. (2004) *Molecular Biology and Evolution* 21, 1214–1225.
28. Hearne, S., Chen, C., Buckler, E., & Mitchell, S. (2015) Unimputed gbs derived snps for maize landrace accessions represented in the seed-maize gwas panel (.). Accessed: 2015-02-16.
29. Schiffels, S. & Durbin, R. (2014) *Nature genetics*.
30. Chia, J.-M., Song, C., Bradbury, P. J., Costich, D., de Leon, N., Doebley, J., Elshire, R. J., Gaut, B., Geller, L., Glaubitz, J. C., et al. (2012) *Nature genetics* 44, 803–807.
31. Panzea. (In prep) TBD.
32. Hufford, M. B., Xu, X., Van Heerwaarden, J., Pyhäjärvi, T., Chia, J.-M., Cartwright, R. A., Elshire, R. J., Glaubitz, J. C., Guill, K. E., Kaeplier, S. M., et al. (2012) *Nature genetics* 44, 808–811.
33. Tenaillon, M. I., Sawkins, M. C., Anderson, L. K., Stack, S. M., Doebley, J., & Gaut, B. S. (2002) *Genetics* 162, 1401–1413.
34. Innan, H. & Kim, Y. (2004) *Proceedings of the National Academy of Sciences of the United States of America* 101, 10667–10672.
35. Messer, P. W. & Petrov, D. A. (2013) *Trends in ecology & evolution* 28, 659–669.
36. Garud, N. R., Messer, P. W., Buzbas, E. O., & Petrov, D. A. (2015) *PLoS genetics* 11, e1005004.
37. Wang, H., Nussbaum-Wagler, T., Li, B., Zhao, Q., Vigouroux, Y., Faller, M., Bomblies, K., Lukens, L., & Doebley, J. F. (2005) *Nature* 436, 714–719.
38. Wang, H., Studer, A. J., Zhao, Q., Meeley, R., & Doebley, J. F. (2015) *Genetics pp. genetics*–115.
39. Enard, D., Messer, P. W., & Petrov, D. A. (2014) *Genome research* 24, 885–895.
40. Rodgers-Melnick, E., Bradbury, P. J., Elshire, R. J., Glaubitz, J. C., Acharya, C. B., Mitchell, S. E., Li, C., Li, Y., & Buckler, E. S. (2015) *Proceedings of the National Academy of Sciences* 112, 3823–3828.
41. Davydov, E. V., Goode, D. L., Sirota, M., Cooper, G. M., Sidow, A., & Batzoglou, S. (2010) *PLoS Comput Biol* 6, e1001025.
42. Studer, A., Zhao, Q., Ross-Ibarra, J., & Doebley, J. (2011) *Nature genetics* 43, 1160–1163.
43. Gallavotti, A., Zhao, Q., Kyozuka, J., Meeley, R. B., Ritter, M. K., Doebley, J. F., Pè, M. E., & Schmidt, R. J. (2004) *Nature* 432, 630–635.
44. Wills, D. M., Whipple, C. J., Takuno, S., Kursel, L. E., Shannon, L. M., Ross-Ibarra, J., & Doebley, J. F. (2013) *PLoS Genet* 9, e1003604.
45. Takuno, S., Ralph, P., Swarts, K., Elshire, R. J., Glaubitz, J. C., Buckler, E. S., Hufford, M. B., & Ross-Ibarra, J. (2015) *Genetics*.
46. Beissinger, T. M., Hirsch, C. N., Vaillancourt, B., Deshpande, S., Barry, K., Buell, C. R., Kaeplier, S. M., Gianola, D., & de Leon, N. (2014) *Genetics* 196, 829–840.
47. Clark, R. M., Tavaré, S., & Doebley, J. (2005) *Molecular biology and evolution* 22, 2304–2312.
48. Eyre-Walker, A. & Keightley, P. D. (2007) *Nature Reviews Genetics* 8, 610–618.
49. Wallace, J., Larsson, S., & Buckler, E. (2014) *Heredity* 112, 30–38.
50. Weber, A. L., Briggs, W. H., Rucker, J., Baltazar, B. M., de Jesus Sánchez-Gonzalez, J., Feng, P., Buckler, E. S., & Doebley, J. (2008) *Genetics* 180, 1221–1232.
51. Pyhäjärvi, T., Hufford, M. B., Mezmouk, S., & Ross-Ibarra, J. (2013) *Genome biology and evolution* 5, 1594–1609.
52. Sattath, S., Elyashiv, E., Kolodny, O., Rinott, Y., & Sella, G. (2011) *PLoS genetics* 7, e1001302.
53. Williamson, R., Josephs, E., Platts, A., Hazzouri, K., Haudry, A., Blanchette, M., & Wright, S. (2014) *PLoS genetics* 10, e1004622–e1004622.
54. Hernandez, R. D., Kelley, J. L., Elyashiv, E., Melton, S. C., Auton, A., McVean, G., Sella, G., Przeworski, M., et al. (2011) *science* 331, 920–924.
55. Pritchard, J. K., Pickrell, J. K., & Coop, G. (2010) *Current Biology* 20, R208–R215.
56. Piperno, D. R., Ranere, A. J., Holst, I., Iriarte, J., & Dickau, R. (2009) *Proceedings of the National Academy of Sciences* 106, 5019–5024.
57. Keinan, A. & Clark, A. G. (2012) *science* 336, 740–743.
58. Program, T. M. (1999) *Development, maintenance, and seed multiplication of open-pollinated maize varieties*. (CIMMYT, Mexico, D.F.), 2 edition.
59. Baden, W. W. & Beekman, C. S. (2001) *American Antiquity* pp. 505–515.
60. Kimura, M. (1984) *The neutral theory of molecular evolution*. (Cambridge University Press).
61. Ross-Ibarra, J., Tenaillon, M., & Gaut, B. S. (2009) *Genetics* 181, 1399–1413.
62. Meghji, M., Dudley, J., Lambert, R., & Sprague, G. (1984) *Crop Science* 24, 545–549.
63. Doebley, J. F., Gaut, B. S., & Smith, B. D. (2006) *Cell* 127, 1309–1321.
64. Zhu, Q., Zheng, X., Luo, J., Gaut, B. S., & Ge, S. (2007) *Molecular Biology and Evolution* 24, 875–888.
65. Larson, G. & Burger, J. (2013) *Trends in Genetics* 29, 197–205.
66. Lemmon, Z. H., Bukiowski, R., Sun, Q., & Doebley, J. F. (2014) *PLoS Genet* 10, e1004745.
67. Jombart, T. & Ahmed, I. (2011) *Bioinformatics* 27, 3070–3071.
68. Schnable, P. S., Ware, D., Fulton, R. S., Stein, J. C., Wei, F., Pasternak, S., Liang, C., Zhang, J., Fulton, L., Graves, T. A., et al. (2009) *science* 326, 1112–1115.
69. Li, H. (2011) *Bioinformatics* 27, 2987–2993.
70. Glaubitz, J. C., Casstevens, T. M., Lu, F., Harriman, J., Elshire, R. J., Sun, Q., & Buckler, E. S. (2014) *PLoS One* 9, E90346.
71. Durinck, S., Spellman, P. T., Birney, E., & Huber, W. (2009) *Nature protocols* 4, 1184–1191.
72. Durinck, S., Moreau, Y., Kasprzyk, A., Davis, S., De Moor, B., Brazma, A., & Huber, W. (2005) *Bioinformatics* 21, 3439–3440.
73. R Core Team. (2014) *R: A Language and Environment for Statistical Computing* (R Foundation for Statistical Computing, Vienna, Austria).
74. Korneliussen, T. S., Albrechtsen, A., & Nielsen, R. (2014) *BMC bioinformatics* 15, 356.
75. Fu, Y.-X. & Li, W.-H. (1993) *Genetics* 133, 693–709.
76. McLaren, W., Pritchard, B., Rios, D., Chen, Y., Flieck, P., & Cunningham, F. (2010) *Bioinformatics* 26, 2069–2070.

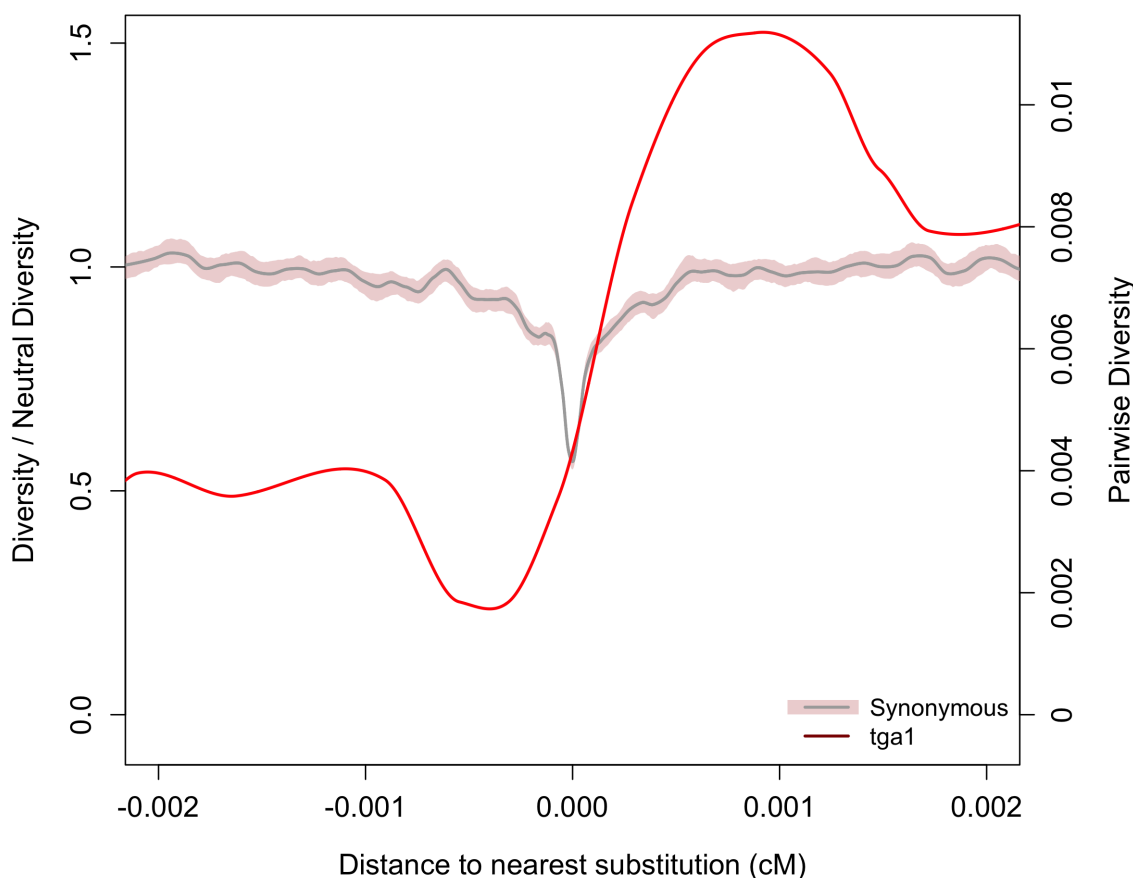


Fig. S1. Diversity surrounding the causitive polymorphism at the *tga1* locus is plotted. Since this is only one gene, the large amount of noise compared to our average plots is expected. However, notice that diversity precisely at the causitive polymorphism is reduced and a recovery of diversity is observed away from that site.

Supporting Information

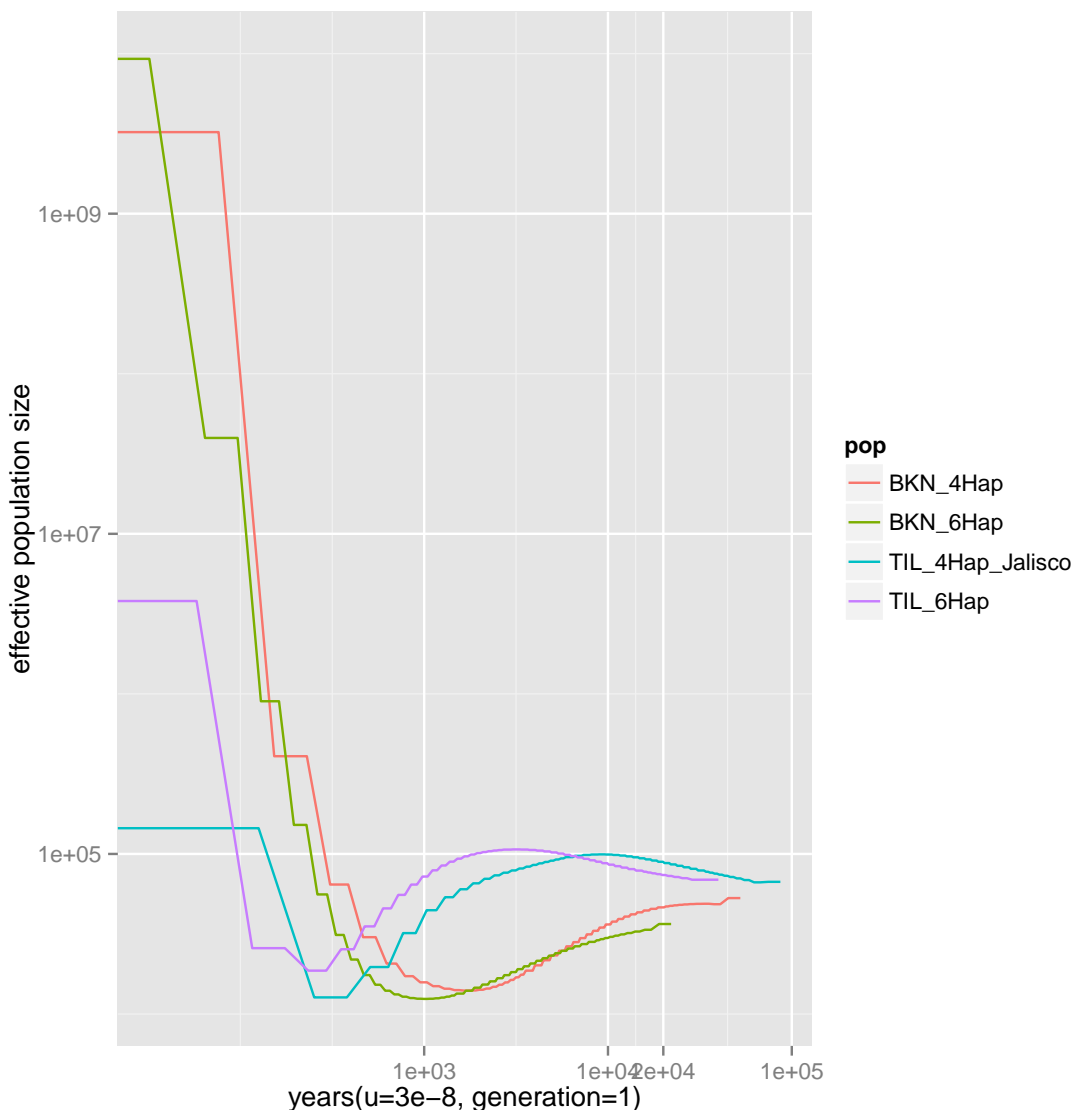


Fig. S2. need MSMC caption

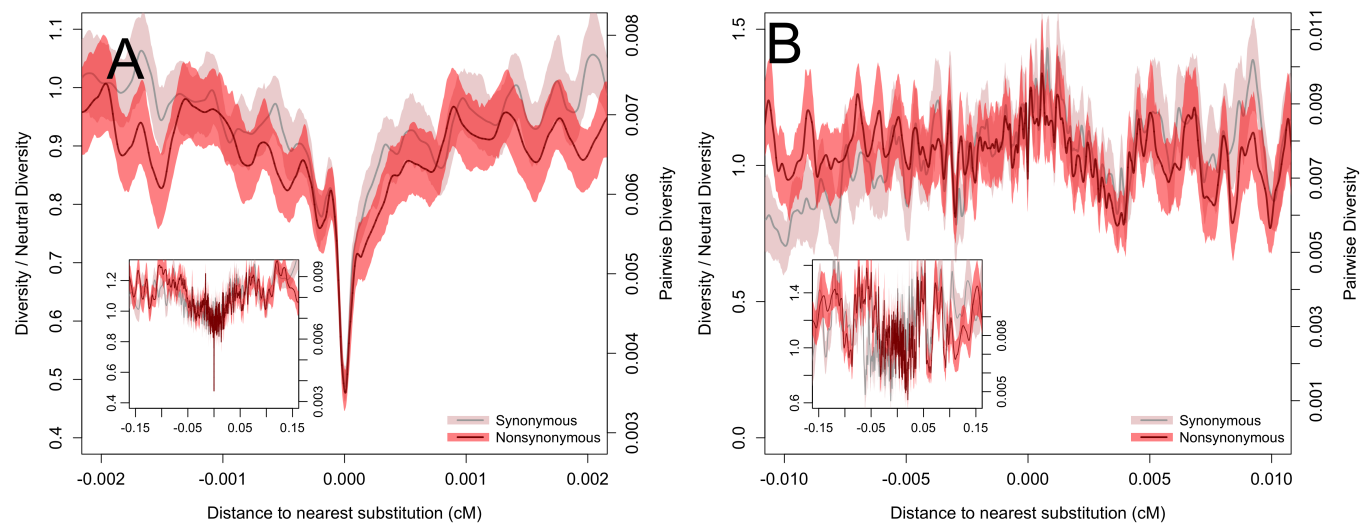


Fig. S3. Pairwise diversity surrounding synonymous and nonsynonymous substitutions in maize at highly conserved (A) or unconserved (B) sites. Bootstrap-based 95% confidence intervals are depicted via shading. Inset plots depict a larger range on the x-axis.

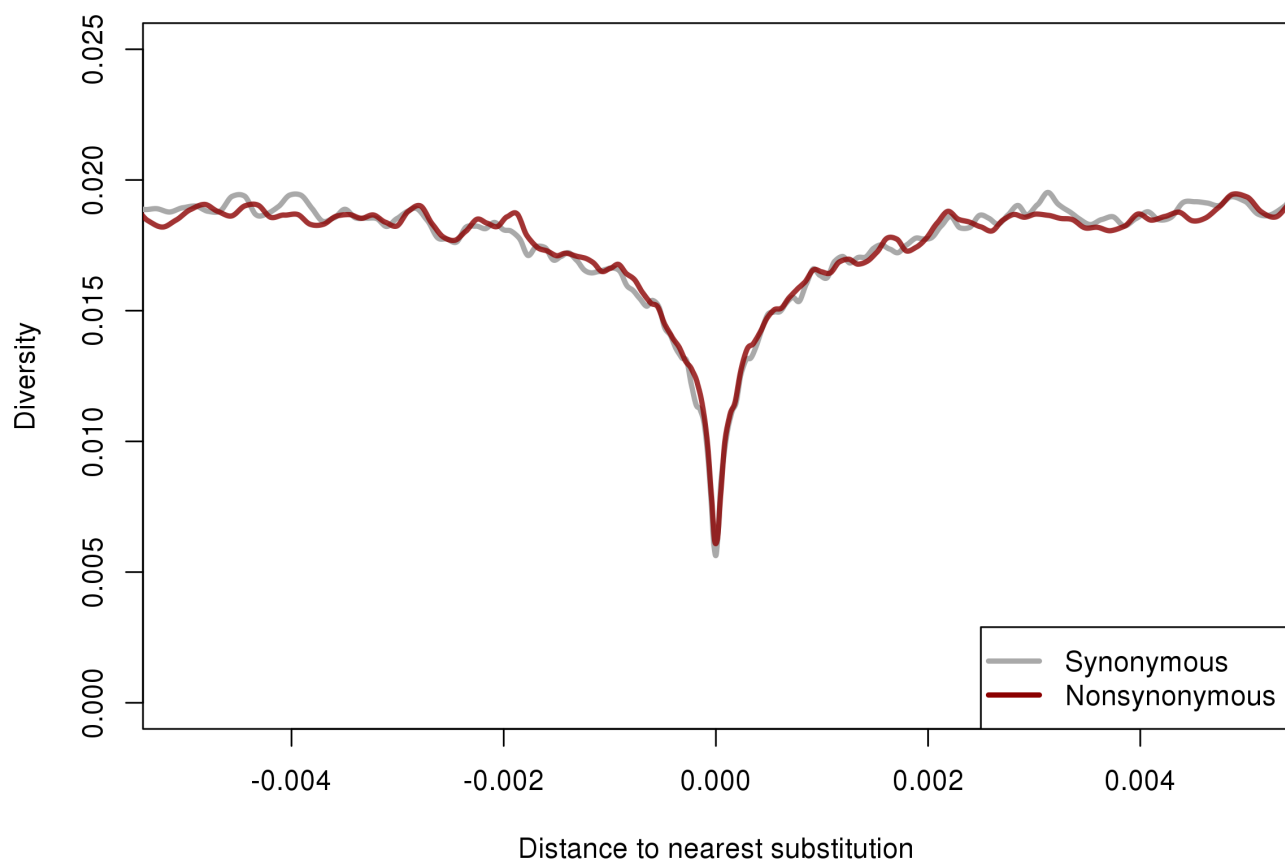


Fig. S4. Singleton diversity surrounding synonymous and nonsynonymous substitutions in maize.

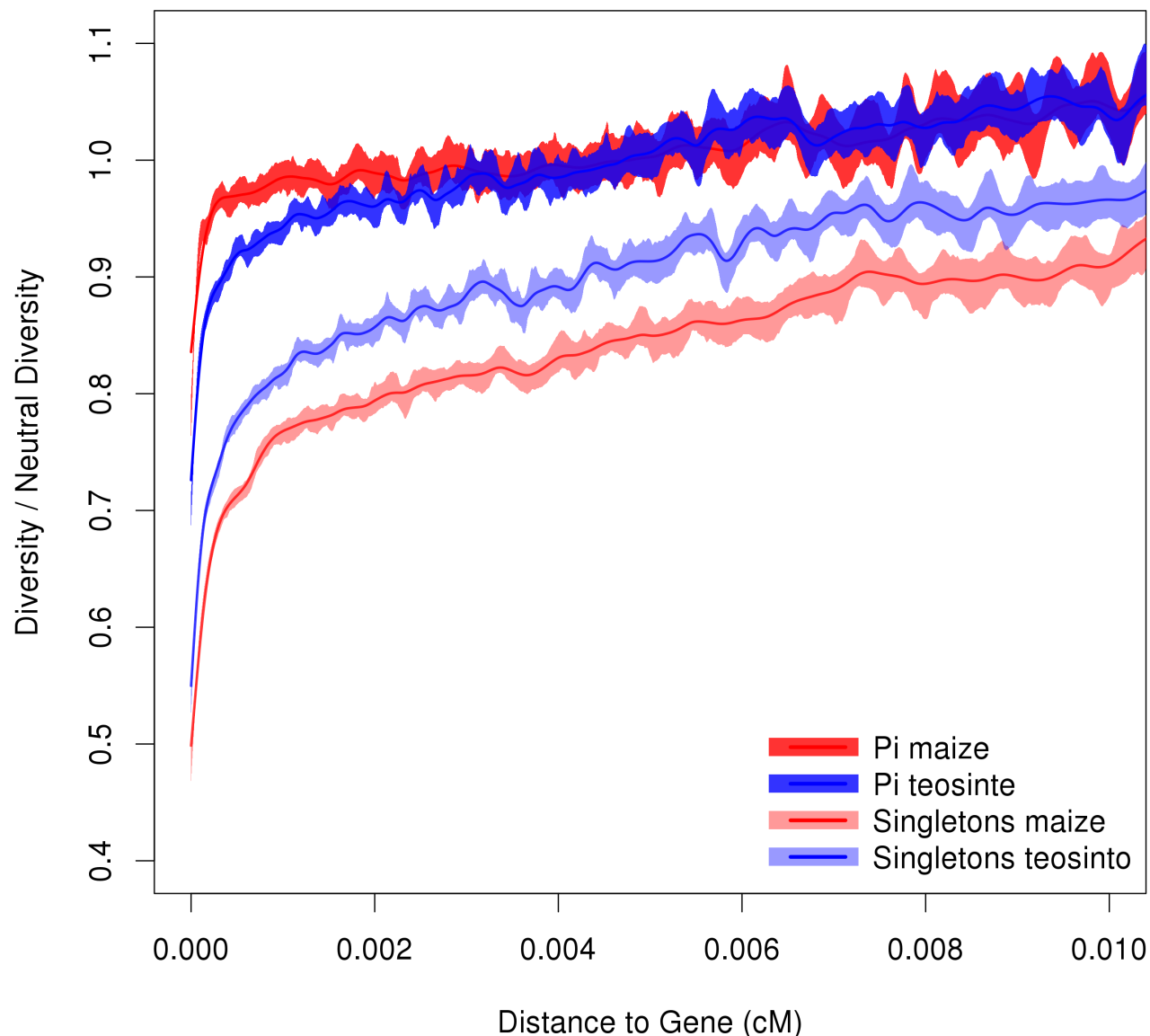


Fig. S5. Relative diversity versus distance to nearest gene in maize and teosinte. Relative diversity is calculated by comparing to the mean diversity in all windows $\geq 0.02\text{cM}$ from the nearest gene. Lines depict cubic smoothing splines with smoothing parameters chosen via generalized cross validation and shading depicts bootstrap-based 95% confidence intervals.

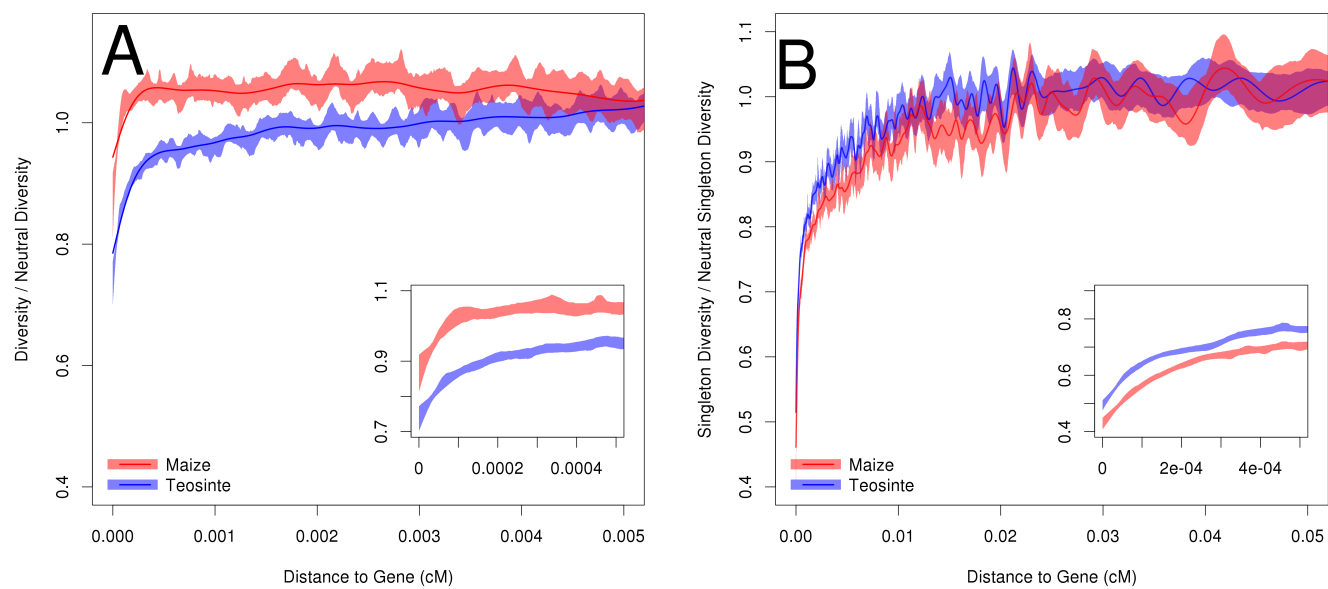


Fig. S6. Relative level of diversity versus distance to the nearest gene, in maize and teosinte, based on only sites that do not show evidence of hard or soft sweeps according to H12. Two measures of diversity were investigated. **A** displays pairwise diversity, which is most influenced by intermediate frequency alleles and therefore depicts more ancient evolutionary patterns, and **B** depicts singleton diversity, influenced by rare alleles and thus depicting evolutionary patterns in the recent past. Bootstrap-based 95% confidence intervals are depicted via shading. Inset plots depict a smaller range on the x-axis.

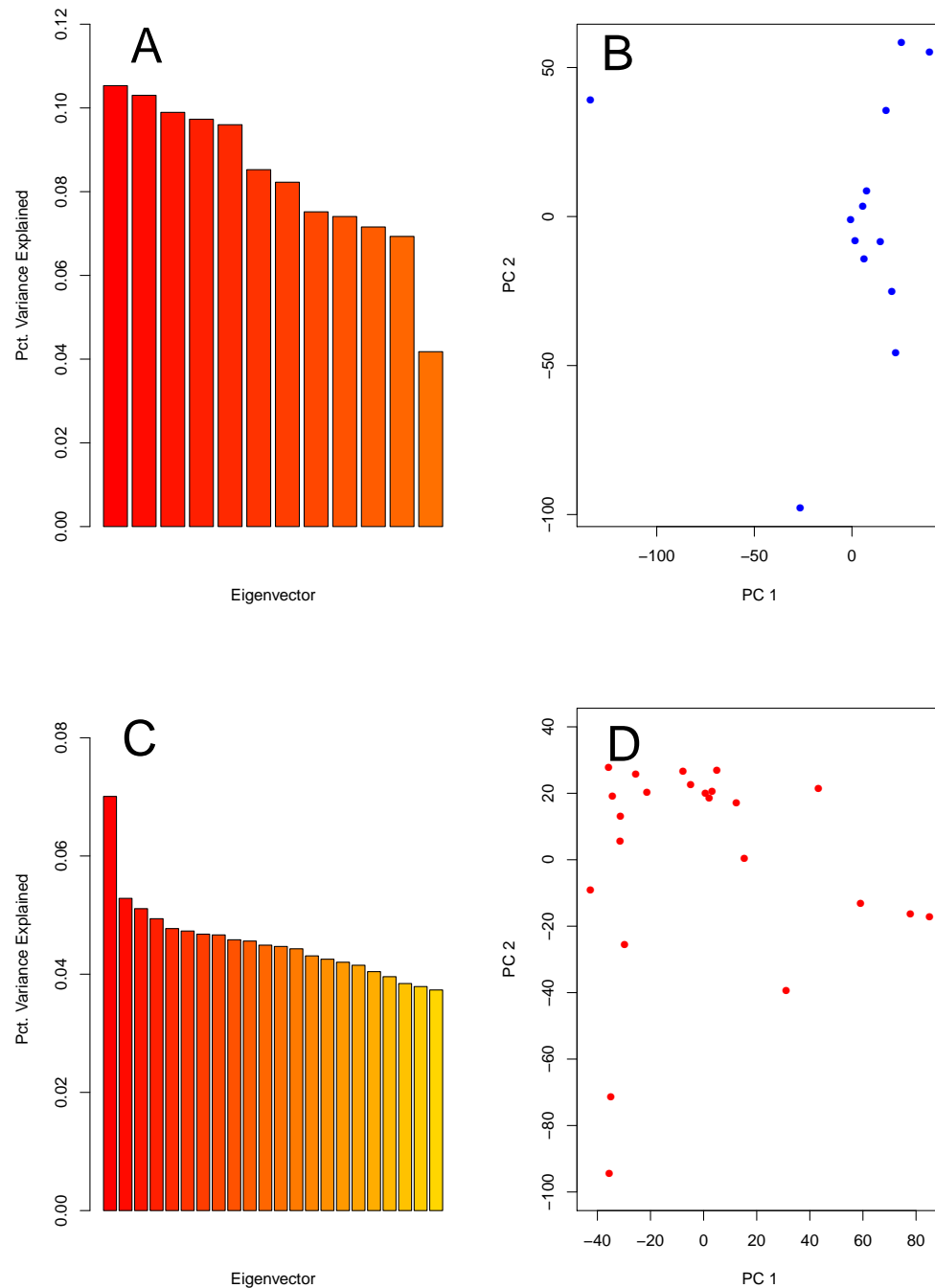


Fig. S7. Principal component analysis of teosinte and maize individuals to ensure that no close relatives were inadvertently included in our study. Plots are based on a random sample of 10,000 SNPs. **A:** Percentage of total variance explained by each principal component for teosinte. **B:** PC1 vs PC2 for all 13 teosinte individuals. **C:** Percentage of total variance explained by each principal component for maize. **D:** PC1 vs PC2 for all 23 maize individuals.

Maize	Teosinte
BKN009	TIL01
BKN010	TIL02
BKN011	TIL03
BKN014	TIL04-TIP454
BKN015	TIL07
BKN016	TIL09
BKN017	TIL10
BKN018	TIL11
BKN019	TIL12
BKN020	TIL14-TIP498
BKN022	TIL15
BKN023	TIL16
BKN025	TIL17
BKN026	
BKN027	
BKN029	
BKN030	
BKN031	
BKN032	
BKN033	
BKN034	
BKN035	
BKN040	

Fig. S8. A list of maize and teosinte individuals included in this study. Sequencing and details were previously described by [cite chia and lemmmon](#)

Parameter	Initial value	Upper bound	Lower bound
$\frac{N_b}{N_a}$	0.02	1×10^{-7}	2
$\frac{N_m}{N_a}$	3	1×10^{-7}	200
$\frac{T_b}{2N_a}$	0.04	0	1
$\frac{M_{mt}}{N_a}$	1×10^{-10}	1×10^{-7}	0.001
$\frac{M_{tm}}{N_a}$	1×10^{-10}	1×10^{-7}	0.001

Fig. S9. Parameters, initial values, and boundaries used for model-fitting with $\delta\alpha\delta i$. Parameters are shown in the units utilized by $\delta\alpha\delta i$, although in the text simplified units are reported.

